Article

Three-Dimensional Energy Transport in Highly Luminescent Host–Guest Crystals: A Quantitative Experimental and Theoretical Study

Lars Poulsen, Mikael Jazdzyk, Jean-Edouard Communal, Juan Carlos Sancho-Garca, Andrea Mura, Giovanni Bongiovanni, David Beljonne, Jrme Cornil, Michael Hanack, Hans-Joachim Egelhaaf, and Johannes Gierschner

J. Am. Chem. Soc., **2007**, 129 (27), 8585-8593• DOI: 10.1021/ja0714437 • Publication Date (Web): 12 June 2007

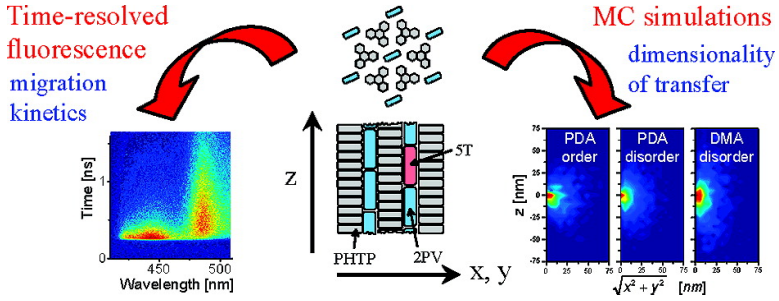

More About This Article

Additional resources and features associated with this article are available within the HTML version:

- Supporting Information
- Links to the 6 articles that cite this article, as of the time of this article download
- Access to high resolution figures
- Links to articles and content related to this article
- Copyright permission to reproduce figures and/or text from this article

View the Full Text HTML

J|A|C|S
ARTICLES
Published on Web 06/12/2007

Three-Dimensional Energy Transport in Highly Luminescent Host−Guest Crystals: A Quantitative Experimental and Theoretical Study

Lars Poulsen,[†] Mikael Jazdzyk,[‡] Jean-Edouard Communal,[§] Juan Carlos Sancho-García,[||] Andrea Mura,[§] Giovanni Bongiovanni,[§] David Beljonne,[||] Jérôme Cornil,[||] Michael Hanack,[‡] Hans-Joachim Egelhaaf,*[,†,⊥] and Johannes Gierschner*[,†,||]

Contribution from the Institute of Physical and Theoretical Chemistry, University of Tübingen, Auf der Morgenstelle 8, D-72076 Tübingen, Germany, Institute of Organic Chemistry, University of Tübingen, Auf der Morgenstelle 18, D-72076 Tübingen, Germany, Dipartimento di Fisica and Istituto Nazionale di Fisica della Materia, Università degli Studi di Cagliari, I-09042 Monserrato (CA), Italy, Laboratory for Chemistry of Novel Materials, Center for Research in Molecular Electronics and Photonics, University of Mons-Hainaut, Place du Parc 20, B-7000 Mons, Belgium, and Christian-Doppler Laboratory for Surface Optical Methods, Institute for Semiconductor Physics, Johannes-Kepler-University, Altenbergerstr. 69, Linz, Austria

Received March 1, 2007; E-mail: hegelhaaf@konarka.com; johannes@averell.umh.ac.be

Abstract: We present a combined experimental and theoretical study on energy transfer processes in a well-defined three-dimensional host−guest system, which allows for high chromophore concentrations while maintaining the highly luminescent properties of the molecules in solution. The self-assembled, nanostructured system with a defined ratio of included donor and acceptor molecules is amenable to quantitative comparison between experiment and theory. Experimentally, energy migration is monitored by steady-state and time-resolved fluorescence spectroscopy. From the theoretical side, the energy transfer process is modeled by a Monte Carlo approach including homo and hetero transfer steps with multi-acceptor distribution. In this dense system, the classical Förster point-dipole approach for energy transfer breaks down, and the hopping rates are therefore calculated on the basis of a quantum-chemical description of the donor and acceptor excited states. Thereby, the true directionality of the excitation diffusion is revealed. Excellent agreement with experimental donor and acceptor decays and overall transfer efficiencies is found. Even at low acceptor concentrations (down to 0.1%), efficient energy transfer over distances as large as 25 nm was observed due to rapid energy migration through a series of homo-transfer steps with preference along one direction of the structure.

1. Introduction

Resonance energy transfer is a key issue in many photophysical processes ranging from solar energy harvesting to white light-emitting diodes (LEDs) and has found use as a valuable tool for determining molecular distances in biological systems. Furthermore, energy transfer plays an important part in the photophysics of chromophore aggregates and organic conducting polymers because it affects the excitation dynamics and leads to effects like enhanced energy trapping at defect sites, emission depolarisation, and singlet−singlet annihilation.[1,2] Recently, multi-chromophoric systems with a high degree of order have drawn the attention of us and others.[3−13] These systems are model systems to study fundamental questions related to excitation transport such as diffusion lengths, energy migration dynamics, and directionality. A special class of such highly ordered systems are the so-called nanochannel compounds. Here, the chromophores are embedded in channel-forming organic or inorganic host systems such as organic crystals (e.g., perhy-

[†] Institute of Physical and Theoretical Chemistry, University of Tübingen.
[‡] Institute of Organic Chemistry, University of Tübingen.
[§] Università degli Studi di Cagliari.
[||] University of Mons-Hainaut.
[⊥] Johannes-Kepler-University.

(1) Scholes, G. D. *Ann. Rev. Phys. Chem.* **2003**, *54*, 57.
(2) Egelhaaf, H. J.; Gierschner, J.; Oelkrug, D. *Synth. Met.* **2002**, *127*, 221.
(3) Komorowska, K.; Brasselet, S.; Dutier, G.; Ledoux, I.; Zyss, J.; Poulsen, L.; Jazdzyk, M.; Egelhaaf, H.-J.; Gierschner, J.; Hanack, M. *Chem. Phys.* **2005**, *318*, 12.
(4) Wiesenhofer, H.; Beljonne, D.; Scholes, G. D.; Hennebicq, E.; Brédas, J. L.; Zojer, E. *Adv. Funct. Mater.* **2005**, *15*, 155.
(5) Beljonne, D.; Hennebicq, E.; Daniel, C.; Herz, L. M.; Silva, C.; Scholes, G. D.; Hoeben, F. J. M.; Jonkheijm, P.; Schenning, A.; Meskers, S. C. J.; Phillips, R. T.; Friend, R. H.; Meijer, E. W. *J. Phys. Chem. B* **2005**, *109*, 10594.
(6) Calzaferri, G.; Huber, S.; Maas, H.; Minkowski, C. *Angew. Chem., Int. Ed.* **2003**, *42*, 3732.
(7) Sancho-Garcia, J. C.; Brédas, J. L.; Beljonne, D.; Cornil, J.; Martinez-Alvarez, R.; Hanack, M.; Poulsen, L.; Gierschner, J.; Mack, H. G.; Egelhaaf, H. J.; Oelkrug, D. *J. Phys. Chem. B* **2005**, *109*, 4872.
(8) Gierschner, J.; Egelhaaf, H. J.; Mack, H. G.; Oelkrug, D.; Martinez Alvarez, R.; Hanack, M. *Synth. Met.* **2003**, *137*, 1449.
(9) Sancho-Garcia, J. C.; Poulsen, L.; Gierschner, J.; Martinez-Alvarez, R.; Hennebicq, E.; Hanack, M.; Egelhaaf, H.-J.; Oelkrug, D.; Beljonne, D.; Brédas, J.-L.; Cornil, J. *Adv. Mater.* **2004**, *16*, 1193.
(10) Minkowski, C.; Calzaferri, G. *Angew. Chem., Int. Ed.* **2005**, *44*, 5325.

drotriphenylene, urea, tris-o-phenylenedioxycyclotriphosphazene) or zeolites, which results in controlled geometries with weak interchromophore interactions.

The present paper focuses on organic nanochannel compounds based on the host material perhydrotriphenylene (PHTP). In the presence of suitable guest molecules, such as rod-shaped, π-conjugated chromophores or small solvent molecules, PHTP self-assembles into a nanostructured pseudo-hexagonal host-lattice with completely filled parallel channels (Figure 1).[14,15] Chromophores included in the PHTP channels are thus all oriented parallel in a head-to-tail configuration. Despite their high concentrations (~0.5 M), fluorescence spectra, quantum yields and lifetimes of chromophores included in PHTP resemble those of the chromophores in solution, implying that the distance between adjacent channels of approximately 1.5 nm is long enough to prevent strong side-by-side interactions, which usually lead to fluorescence quenching.[2,13] Previous studies have shown that upon doping of inclusion compounds with an appropriate energy acceptor, excitation energy is transferred efficiently to the dopant.[13,16] In the present study, distyrylbenzene (2PV) and quinquethiophene (5T) will be used as the energy donating and energy accepting species, respectively.

The well-defined geometry of PHTP allows for a unique possibility to compare experimental data on three-dimensional energy migration with simulations based on different models. Of particular interest in this context is the issue of accurate description of the individual energy transfer steps at small interchromophore distances where the classical Förster theory, based on point-dipole interactions (the Point Dipole Approximation, PDA),[17] is no longer applicable and the full electronic transition density distribution on the molecules must be taken into account.[1] This issue will be addressed at a quantum-chemical level based on the distributed monopole approach (DMA), which has been previously validated for systems lying in the weak coupling limit, as it is the case here.[9,18] By accounting for the electronic interactions between the chromophores at the atomistic level, a microscopic picture for the ordered multiple acceptor energy transfer system is achieved. We will compare the results obtained by this approach to those predicted from simple, approximate analytical models, which ignore orientational effects and/or acceptor distribution heterogeneities by assuming rotational averaging (as typically found in liquid solutions) or assume rapid excitation diffusion by means of homo-transfer, i.e., energy transfer between species of the energy donor type (the rapid-diffusion limit),[19] respectively.

Methods of numerical simulation for energy diffusion in the weak coupling limit generally fall into two categories: the Pauli Master Equation approach (or Markov Chain Approach)[20−22] and the Monte Carlo approach.[23−25] In the former, a lattice of chromophores is generated and the time evolution of the excitation probability distribution is solved for all lattice sites yielding a matrix problem of dimension $n \times n$, where n is the number of lattice sites. Thus, this is the method of choice in systems with high order and symmetry, where small lattices

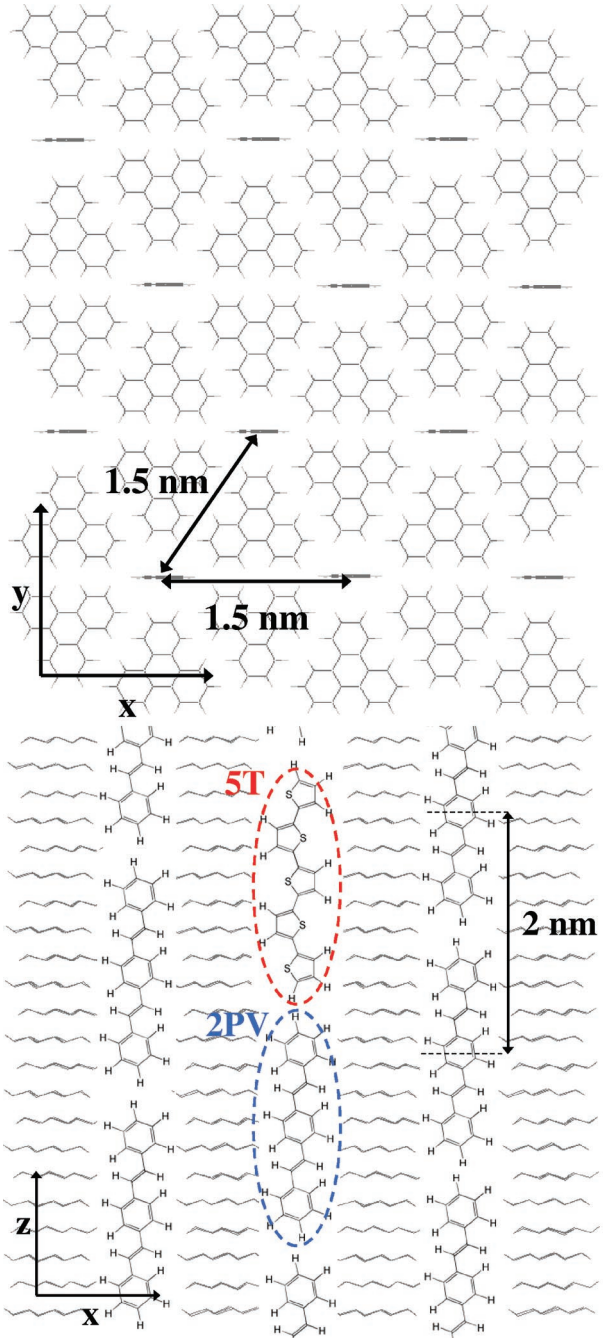

Figure 1. Structure of the PHTP/2PV/5T inclusion compound. (Top) Top view of the hexagonal arrangement of the channels with the *inter*channel distance of 1.5 nm used in the simulations indicated. (Bottom) Side view of the channels with the *intra*channel distance of 2 nm indicated. The structure of molecules of the donor species, 2PV, and of the acceptor species, 5T, are shown in the figure.

(11) Botta, C.; Patrinoiu, G.; Picouet, P.; Yunus, S.; Communal, J.-E.; Cordella, F.; Quochi, F.; Mura, A.; Bongiovanni, G.; Pasini, M.; Destri, S.; Di Silvestro, G. *Adv. Mater.* **2004**, *16*, 1716.
(12) Kim, O.-K.; Je, J.; Melinger, J. S. *J. Am. Chem. Soc.* **2006**, *128*, 4532.
(13) Gierschner, J.; Lüer, L.; Oelkrug, D.; Musluoğlu, E.; Behnisch, B.; Hanack, M. *Synth. Met.* **2001**, *121*, 1695.
(14) Farina, M.; Di Silvestro, G.; Sozzani, P. *Compr. Supramol. Chem.* **1996**, *6*, 371.
(15) Koenig, O.; Buergi, H.-B.; Armbruster, T.; Hulliger, J.; Weber, T. *J. Am. Chem. Soc.* **1997**, *119*, 10632.
(16) Bongiovanni, G.; Botta, C.; Communal, J. E.; Cordella, F.; Magistrelli, L.; Mura, A.; Patrinoiu, G.; Picouet, P.; Di-Silvestro, G. *Mater. Sci. Eng., C* **2003**, *23*, 909.
(17) Förster, T. *Fluoreszenz organischer Verbindungen*; Vandenhoeck & Ruprecht: Göttingen, 1951.
(18) Beljonne, D.; Cornil, J.; Silbey, R.; Millié, P.; Brédas, J.-L. *J. Chem. Phys.* **2000**, *112*, 4749.
(19) Lakowicz, J. R. *Principles of Fluorescence Spectroscopy*, 2nd ed.; Kluwer Academic/Plenum Publishers: New York, 1999.
(20) Bongiovanni, G.; Botta, C.; Di, Silvestro, G.; Loi, M. A.; Mura, A.; Tubino, R. *Chem. Phys. Lett.* **2001**, *345*, 386.
(21) Gfeller, N.; Calzaferri, G. *J. Phys. Chem. B* **1997**, *101*, 1396.

can be chosen. However, for problems where inhomogeneities (e.g., lattice disorder or inhomogeneous trap distributions) are present and when steady-state properties are sought after, long simulations on very large lattices may be needed to give an accurate description of the whole system. In the approach used in this paper, the chromophore lattice is sampled according to a Monte Carlo scheme yielding the trajectories of individual excitations. By introducing cutoff distances for the calculation of energy transfer rates, very large lattices with dimensions comparable to real crystal dimensions can be explored. This opens up the possibility to examine systems with low and inhomogeneous acceptor distributions and to elucidate the mechanism of energy transport in three-dimensional condensed systems.

2. Theoretical Background on Energy Transfer

2.1. Rate Constants. The rate of resonance energy transfer from an energy donating molecule, D, to an energy accepting molecule, X, can be obtained from Fermi's Golden Rule

$$k_{ET}(DX) = \frac{2\pi}{\hbar} |V_{DX}|^2 \cdot J'_{DX} \tag{1}$$

where V_{DX} is the electronic coupling between the initial state (D*X) and the final state (DX*) and J'_{DX} is the spectral overlap between donor emission and acceptor absorption spectra, both area-normalized on an energy scale.[1] The energy accepting molecule, X, can either be of the donor species, X = D, (homo-transfer) or of the acceptor species, X = A (hetero-transfer).

For large separations of the energy donating and the energy accepting molecule, Förster's classic point-dipole approximation (PDA) is sufficient for describing the energy transfer process. Using Förster's formalism,[17] eq 1 can be written as:

$$k_{ET}(DX) = \frac{9 \cdot \ln 10}{128 \cdot \pi^5 \cdot N_A} \cdot k_{F,D} \cdot \frac{1}{n^4} \cdot \frac{\kappa^2_{DX}}{R^6_{DX}} \cdot J_{DX} \tag{2}$$

Here N_A is the Avogadro constant, $k_{F,D} = \Phi_D/\tau_D$ is the rate constant for donor emission, Φ_D and τ_D are the donor fluorescence quantum yield and lifetime, respectively (all in the absence of energy transfer), and n is the refractive index of the medium. The correct description of the dielectric screening by the medium is a non-trivial issue.[1,26] It becomes especially difficult in the present system due to its anisotropy and the high concentration of chromophores. However, keeping in mind that the chromophores in the host−guest system are only weakly coupled, Förster's expression appears as a reasonable approximation.[27]

The spectral overlap J_{DX} is given by the overlap between the area-normalized fluorescence emission spectrum, f_D, of the energy-donating molecule, D, and the absorption spectrum, ϵ_X, of the energy accepting molecule, X:

$$J_{DX} = \int_0^\infty \frac{f_D(\nu) \cdot \epsilon_X(\nu)}{\nu^4} d\nu \tag{3}$$

κ_{DX} is the orientation factor describing the relative orientation of the two transition dipole moments. The transition dipole moments of 5T as 2PV[28] are oriented mainly along its long molecular axis and thus, almost parallel to the PHTP channels. For parallel orientation of the dipole moments, the expression for κ_{DX} reduces to:

$$\kappa_{DX} = 1 - 3\cos^2\theta \tag{4}$$

where θ is the angle between the transition dipole moment and the vector connecting the centers of the molecules (R_{DX}). Because the PHTP host-structure offers a well-defined geometry, the orientation factor can be explicitly calculated for all DX pairs in the system. Note that κ^2_{DX} takes on the value of 1 for *inter*channel transfer when the vector connecting the centers of the molecules is perpendicular to the channel axis and the value of 4 for *intra*channel transfer.

For smaller intermolecular separations, the point-dipole approximation, used in eq 2, breaks down, and the electronic coupling V_{DX} in eq 1 has to be calculated explicitly. In a previous study,[9] we have applied the distributed monopole approach (DMA) to calculate V_{DX}:[29,30]

$$V_{DX} = \frac{1}{4\pi\epsilon_0} \sum_i \sum_j \frac{q_D(i) q_X(i)}{R_{DX}(i,j)} \tag{5}$$

where the atomic transition densities, q, are determined from a ZINDO/S (Zerner's spectroscopic parametrization for the semi-empirical Hartree−Fock intermediate neglect of differential overlap method)[31] calculation of a DX pair, based on geometries optimized at the semiempirical AM1 (Austin Model 1)[32] level, and $R_{DX}(i,j)$ is the distance between atom i in molecule D and atom j in molecule X. In the present study, the DMA approach will be used to calculate directly the orientation factor κ^2_{DX}/R^6_{DX} which enters the Förster equation (eq 2) for transfer steps between molecules in close proximity.[33]

2.2. Common Models of Energy Transfer. As a consequence of the complexity of the energy transfer processes in three-dimensional systems, analytical expressions for the overall rate and yield of energy transfer in an ensemble of multiple energy donating and accepting chromophores are only available for a few special cases. Thus, even within the PDA approach, energy transfer processes are commonly modeled with a number of approximations reducing either the structural or the dynamical

(22) Vega-Duran, J. T.; Diaz-Torres, L. A.; Barbosa-Garcia, O.; Meneses-Nava, M. A.; Mosino, J. F. *J. Luminesc.* **2000**, *91*, 233.
(23) Demidov, A. A. In *Resonance Energy Transfer*; Andrews, D. L., Demidov, A. A., Eds.; John Wiley & Sons: Chichester, 1999.
(24) Yatskou, M. M.; Meyer, M.; Huber, S.; Pfenniger, M.; Calzaferri, G. *ChemPhysChem* **2003**, *4*, 567.
(25) Loura, L. M. S.; Prieto, M. *J. Phys. Chem. B* **2000**, *104*, 6911.
(26) Scholes, G. D.; Curutchet, C.; Mennucci, B.; Cammi, R.; Tomasi, J. *J. Phys. Chem. B*, published online June 6, 2007 http://dx.doi.org/10.1021/jp072540p.
(27) More elaborate description of the dielectric screening than the $1/n^4$ term in the Förster formula involves the correct shape of the molecular cavity as well as the distance dependence of the screening.[26] It becomes even more difficult in the present system due to the anisotropy of the PHTP host, and the high concentration of chromophores, which changes the "effective polarizability" of the medium. However looking at the polarizability tensor of PHTP, the anisotropy turns out to be rather weak, and also the change in the "effective polarizability" is estimated to be rather small. Moreover, keeping in mind, that the chromophores in the host-guest system are only weakly coupled, the distance dependence should be weak. Last but not least, the shape factor for rod-shaped molecules is expected to change the screening by less then 10% compared to Försters formulation.[26]
(28) Gierschner, J.; Ehni, M.; Egelhaaf, H.-J.; Milián-Medina, B.; Beljonne, D.; Benmansour, H.; Bazan, G. C. *J. Chem. Phys.* **2005**, *123*, 144914.
(29) Krueger, B. P.; Scholes, G. D.; Fleming, G. R. *J. Phys. Chem. B* **1998**, *102*, 5378.
(30) Marguet, S.; Markovitsi, D.; Millie, P.; Sigal, H.; Kumar, S. *J. Phys. Chem. B* **1998**, *102*, 4697.
(31) Zerner, M. C. In Reviews, in Computational Chemistry; Boyd, D. B., Ed.; Wiley VCH: New York, 1994; Vol. II, p 313.
(32) Dewar, M. J. S.; Zoebish, E. G.; Healy, E. F.; Stewart, J. J. P. *J. Am. Chem. Soc.* **1985**, *107*, 3902.

complexity. Central in the correct handling of structure is the orientation factor, κ_{DX}. In liquids, the rotational motion of small chromophores can usually be taken to be infinitely faster than the donor decay leading to an averaging of the orientation factor in the Förster equation to $\kappa^2_{DX} = 2/3$. If, on the other hand, the motion of the chromophores is frozen, but the distribution of orientations kept isotropic, κ^2_{DX} averages to 0.476, yielding a smaller overall transfer rate constant.[1,19]

A measure for the efficiency of energy transfer between a given pair of energy donating and energy accepting molecules is the Förster radius, R_0. Assuming fast rotational motion (i.e., $\kappa^2_{DX} = 2/3$), R_0 is the distance at which half of the energy donating molecules transfer their energy to an energy accepting molecule. Complying with the notation given in eq 2, R_0 can be expressed as:

$$R_0^6 = \frac{9 \cdot \ln 10}{128 \cdot \pi^5 \cdot N_A} \cdot \frac{\Phi_D}{n^4} \cdot 2/3 \cdot J_{DX} \qquad (6)$$

The introduction of homo-transfer corresponds to diffusion of the excitation energy (or in the liquid case: the diffusion of the donor molecule) and complicates the treatment of the energy transfer process further. Exact analytical expressions are only available when the diffusion length of the excitation within its lifetime is significantly larger (the rapid-diffusion limit) or smaller (the static limit) than the mean distance between the initially excited donor molecule and an acceptor molecule.[19] In the static limit, homo-transfer can be neglected, but the distribution of transfer distances leads to time-dependent overall energy transfer rate constants and significantly non-exponential donor decays. The analytical expression for the characteristic donor decay in this limit can be written as:[19]

$$I_{DA}^{static} = I_{DA}^{0} \exp\left(-\frac{t}{\tau_D} - \sqrt{\pi}\frac{\rho_A}{\rho_0}\sqrt{\frac{t}{\tau_D}}\right) \qquad (7)$$

where ρ_A is the acceptor density and $\rho_0 = (4/3\pi R_0^3)^{-1}$ is the critical acceptor density related to the Förster radius for hetero-transfer, R_0.

In contrast, in the rapid-diffusion limit, diffusion leads to an averaging of distances so that the overall energy transfer efficiency Φ_{ET} depends only on the molar doping ratio and the shortest possible distances between a donor and acceptor molecule, resulting in single exponential donor decays. For diffusion in three dimensions and spherical molecules, the donor decay takes the following exponential form:[19]

$$I_{DA}^{rapid} = I_{DA}^{0} \exp\left(-\left(\frac{4\pi\rho_A R_0^6}{3r_c^3} + 1\right)\frac{t}{\tau_D}\right) \qquad (8)$$

where r_c is the smallest distance by which a donor and acceptor pair can be separated. In the intermediate domain between the two limits, Φ_{ET} depends on the diffusion coefficient of the excitation and donor decays may be non-exponential.

Numerical simulations allow us to simulate energy transfer processes without the crude approximations that severely limit the applicability of analytical models. Specifically, for systems with complex geometries, distributions of orientation factors, and/or intermediate diffusion rates, numerical simulations are necessary to fully elucidate the dynamics of the energy transfer process. For systems with inherent heterogeneities (in the present case lattice disorder or inhomogeneous trap distributions), very large systems must be sampled in the numerical simulation. Monte Carlo simulations are able to simulate energy transfer in complex molecular assemblies with multiple donors and acceptors using Förster theory[34] or to extract anisotropic energy transfer rate constants by fitting to experimental data.[24,35]

3. Experimental and Computational Methods

3.1. Sample Preparation and Fluorescence Measurements. PHTP/2PV/5T inclusion compounds were prepared by transferring a small amount of 5T solution (in benzene, Merck Spectroscopic grade) to an ampule and then removing the solvent under vacuum. Subsequently, solid PHTP and 2PV were added to the ampule using a large excess of PHTP relative to the ideal PHTP/2PV molar ratio of 9:1.[36] The ampoules were sealed under vacuum and heated to 260 °C. The resulting crystalline powders were smeared onto quartz plates to yield layers of few micrometers, and used for the spectroscopic investigations. UV/vis absorption spectra of solutions were measured on a Perkin-Elmer Lambda2 spectrophotometer. Steady-state fluorescence emission and excitation spectra were recorded at right angle on a SPEX Fluorolog 222 fluorometer equipped with two 0.25 m double monochromators, a 150 W vertical xenon arc-lamp (Müller Electronics) and a photomultiplier tube (Hamamatsu, model R928). Time-resolved fluorescence emission spectra were measured using a femto-second photoluminescence setup consisting of a frequency-doubled Ti:sapphire laser (Spectra Physics, Tsunami) operating at 390 nm with a repetition frequency of 80 MHz and a streak camera (Hamamatsu, C5680) coupled to an imaging monochromator.[11] The excitation light was removed by a 410 nm cutoff filter. To avoid bimolecular processes and sample degradation, the mean laser power was kept below 1 μW.

After determining the desired photophysical properties of the inclusion compounds, the samples were dissolved in benzene and the 2PV and 5T contents were determined using UV/vis absorption and fluorescence emission spectroscopy, respectively. The resulting molar doping ratios, $x_{5T} = n_{5T}/n_{2PV}$, were in the range of 0.001 to 0.04 (i.e., 5×10^{-4} to 2×10^{-2} M). The efficiency of overall energy transfer, Φ_{ET}, from 2PV to 5T is defined as the fraction of the photons absorbed by 2PV transferred to 5T. Assuming steady-state conditions, Φ_{ET} can be determined from the ratio between the integrated fluorescence intensities of 2PV, I_{2PV}, and 5T, $I_{5T,}$ upon selective excitation of 2PV in a 2PV/5T/PHTP sample:

$$\Phi_{ET} = \left(1 + \frac{\Phi_{5T}}{\Phi_{2PV}} \cdot \frac{I_{2PV}}{I_{5T}}\right)^{-1} \qquad (9)$$

where Φ_{5T} and Φ_{2PV} are the fluorescence yields of pure 5T/PHTP and 2PV/PHTP samples, respectively. The contribution to I_{5T} by direct excitation of 5T was estimated to be less than 0.5% of I_{2PV} for molar doping ratios smaller than 0.04 and can therefore be neglected. In time-

(33) For a given intermolecular separation between two identical molecules (X = D) the electronic coupling element V_{DX} is related to the orientation factor κ by the following expression

$$\frac{\kappa_{DX}}{R_{DX}^3} = \frac{32\,\pi^3 \cdot \epsilon_0 \cdot m_e}{3 \cdot e^2} \cdot \frac{\nu_D}{f_D} \cdot V_{DX}$$

where f_D and ν_D are the calculated oscillator strength and the frequency of the electronic transition, respectively. This allows for a perfect match of the DMA results with the PDA model for long intermolecular separations.

(34) Minkowski, C.; Pansu, R.; Takano, M.; Calzaferri, G. *Adv. Funct. Mater.* **2006**, *16*, 273.
(35) Yatskou, M. M.; Donker, H.; Novikov, E. G.; Koehorst, R. B. M.; Van Hoek, A.; Apanasovich, V. V.; Schaafsma, T. J. *J. Phys. Chem. A* **2001**, *105*, 9498.
(36) Gierschner, J.; Lüer, L.; Oelkrug, D.; Musluoğlu, E.; Behnisch, B.; Hanack, M. *Adv. Mater.* **2000**, *12*, 757.

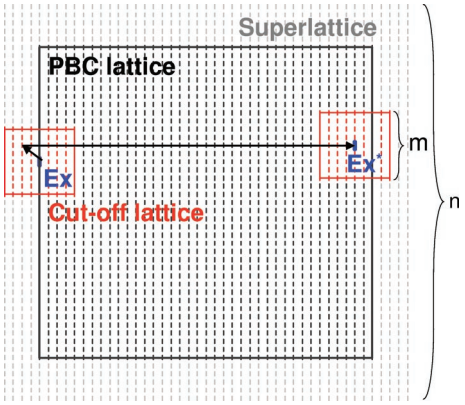

Figure 2. 2D illustration of the lattices used in the Monte Carlo simulation. The excitation, EX, moves on the large superlattice (dimension n^2). Rate constants for energy transfer are only calculated within the cutoff lattice (dimension m^2) with is centered at EX. If an excitation moves to a site outside the PBC lattice (dimension $(n\text{-}m\text{-}1)^2$, it is translated to the equivalent site, EX*, on the other side of the PBC lattice as indicated by the arrows.

resolved experiments, Φ_{ET} can, in the case of exponential decays, be determined from the reduction in the donor lifetime due to energy transfer:

$$\Phi_{ET} = 1 - \tau_{2PV/5T}/\tau_{2PV} \tag{10}$$

where $\tau_{2PV/5T}$ and τ_{2PV} are the donor lifetimes in the presence and absence of the acceptor, respectively.

3.2. Monte Carlo Algorithm. In the MC simulations, the structure of the PHTP/2PV/5T inclusion compound is initially represented by a perfect hexagonal lattice in which each lattice site is occupied by a chromophore with its transition dipole moment oriented along the *z*-axis (Figure 2).[28] At a later stage, random positional disorder along the *z*-axis will be introduced to mimic the real structure (section 4.2). A superlattice consisting of n^3 sites is built and serves as the three-dimensional map on which the excitation moves along the Monte Carlo trajectories. All sites in this superlattice are labeled with a tag defining the site as either a donor (D) or an acceptor (A). The ratio between the number of donor sites, N_D, and the number of acceptor sites, N_A, is the molar doping ratio, x_{5T}. The acceptor sites are randomly distributed in the superlattice leading to a distribution of acceptor−acceptor distances.

For a given position of an excitation, energy transfer rate constants to all donor sites, k_{DD}, and all acceptor sites, k_{DA}, in the superlattice need, in principle, to be calculated in order to determine the excitation motion. To minimize the computational cost of this operation, a smaller cutoff lattice of dimension m^3 is introduced with the excitation placed in the center. The size of the cutoff lattice is chosen so that energy transfer to sites outside of the cutoff lattice is negligible. Thus, it is only necessary to calculate rate constants within the cutoff lattice. Periodic boundary conditions (PBC) are introduced by a third sub-lattice of dimension $(n-m-1)^3$ centered at the same position as the superlattice.[37]

The first step of the algorithm (Figure 3) is to place an excitation, i.e., an excited donor, at a random donor site in the PBC lattice. We label this site "Ex". The time at which the excitation is placed is $t = 0$. From "Ex", the excitation can decay by either normal radiative or nonradiative deactivation ($k_{decay} = k_{fl} = t_D^{-1}$) or by resonance energy

(37) The dimension is chosen such that, providing the excitation is within the PBC lattice, all sites in the cut-off lattice will still be present in the superlattice. If the excitation moves outside the PBC lattice, the excitation is moved to the corresponding site on the opposite side of the PBC lattice. This method of applying periodic boundary conditions is not exact, because the acceptor distribution and any interchannel disorder are not reproduced at the new site. However, for sufficiently large superlattices artifacts thus introduced are negligible. To ensure that the local structure of the superlattice is always matched by the two sub-lattices, two tables are created to translate the number labels between the lattices.

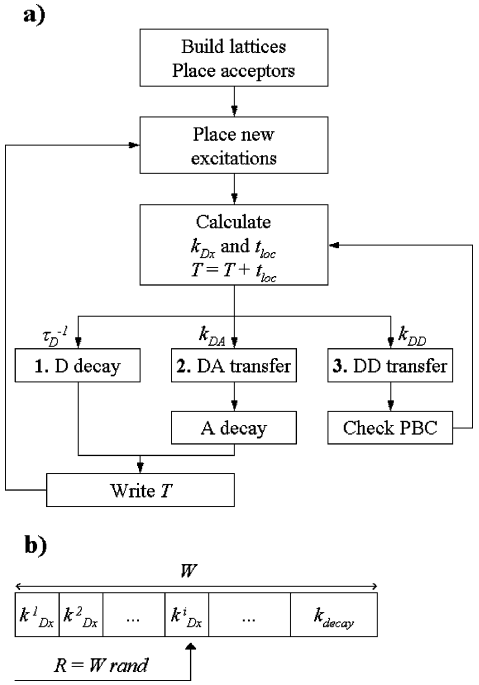

Figure 3. Schematic representation of (a) the Monte Carlo algorithm and (b) the procedure for determining the decay path of the excitation.

Table 1. Summary of the Experimental Photophysical Properties of 2PV and 5T in PHTP[a]

	2PV	5T
ν_{ex} (A_{max}) [cm^{-1}]	27550	22570
ν_{em} (F_1) [cm^{-1}]	25450	20580
Φ_F	0.9	0.3[b]
τ_F [ns]	1.5	0.9
ϵ_{max} [cm^{-1} L mol^{-1}]	6.3×10^4	4.3×10^4[b]
J_{DX} [nm^6 mol^{-1}]	1×10^{31}	1×10^{32}
R_0 [nm]	3.3	4.9

[a] The positions of the absorption maximum, A_{max}, and the F_1 band of the fluorescence emission spectrum are indicated in Figure 5. Fluorescence yields, Φ_F, were determined in cyclohexane against a 9,10-diphenylanthracene standard. Absorption coefficients, ϵ_{max}, were determined in 1,4-dioxane. Overlap integrals, J_{DX}, for 2PV-2PV and 2PV-5T were determined from fluorescence emission and excitation spectra in PHTP at 293 K by eq 3. The Förster radii, R_0, for homo-transfer (2PV/2PV) and hetero-transfer (2PV/5T) were calculated from the tabulated data using an average orientation factor $\kappa^2_{DX} = 2/3$ and $n = 1.4$ (eq 6). [b] From ref 39.

transfer to any donor or acceptor site in the lattice ($k_{decay} = k_{DX}$). The energy transfer rate constants to sites within the cutoff lattice are calculated using either the point-dipole model for all sites (eq 2, results labeled MC PDA) or the point-dipole model combined with rate constants calculated by DMA for nearest neighbors (eq 5, results labeled MC DMA). In the case of the PDA, distances, R_{DX}, and orientation factors, κ_{DX}, are calculated from the lattice model, while other values required for the calculation of the rate constants are taken from Table 1 (J_{DX}, Φ_D, τ_D, n). To feed the MC simulations, hopping rate constants are first calculated at the quantum-chemical level for a grid of chromophore pairs differing in their relative distances and orientations along the same channel as well as in between neighboring channels (Figure 4); these were then interpolated with fourth and sixth degree polynomials to account for intra- and interchannel transfer, respectively.

The rate constant for the decay of the excitation at the site "Ex" is given by the sum of all rate constants:

$$W = \sum_{M_D} k^i_{DD} + \sum_{M_A} k^j_{DA} + k_{fl} \tag{11}$$

where k_{fl} is the rate constant for donor decay in the absence of energy

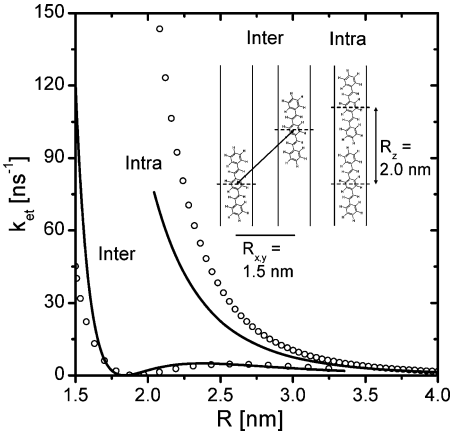

Figure 4. Energy transfer rate constants for a 2PV-2PV pair calculated at the quantum mechanical level using the supramolecular approach (○) and Förster point-dipole approximation (line) for both *intra-* and *inter*channel transfer. The center-to-center distances are indicated by the arrows for both cases.

transfer and M_D and M_A are the numbers of donor and acceptor molecules in the cutoff lattice, respectively. Thus, W^{-1} is the mean lifetime of the excitation at site "Ex".

In the second step, the actual time the excitation is located at the site is determined by a random function as proposed by Demidov:[23]

$$t_{loc} = -W^{-1} \ln(rand) \qquad (12)$$

where *rand* is a random number between 0 and 1. Consequently, the time steps of the algorithm are variable and not subject to any imposed restrictions. The time is now updated to $t = t + t_{loc}$. The third step determines what happens to the excitation after t_{loc}. This is done by lining up the rate constants and using a random number, $R = W\,rand$, to point to the decay path (Figure 3). The excitation may:

(1) Decay by radiative or nonradiative deactivation, in which case the time, *t*, is written to a file and a new excitation is placed in the PBC lattice and the outer loop is repeated.

(2) Jump to an acceptor site, from which it will decay after the time $t_{loc} = -\tau_A \ln(rand)$, where *rand* is a new random number, and the time $t = t + t_{loc}$ is written to a file.

(3) Jump to another donor site.

In the latter case, a check is performed to see if the target donor site is within the PBC lattice. If the target site is outside the PBC lattice, the excitation is moved to the corresponding site on the opposite side of the PBC lattice. The simulation procedure is repeated until smooth time traces are obtained and the energy transfer efficiency has converged (typically a few thousand decays).

The system was checked for size effects by varying the size of the superlattice and cutoff lattice. Due to the use of a cutoff lattice, the total simulation time is insensitive to the superlattice size but scales cubically with the side length of the cutoff lattice. Thus, a large superlattice with 99 × 99 × 99 sites was chosen to minimize the use of PBC conditions. The size of the cutoff lattice was increased until energy transfer to sites at the periphery of the cutoff lattice could no longer be observed. Under all the reported conditions, a cutoff lattice with 11 × 11 × 11 sites was found to be sufficiently large. Even the use of cutoff lattices as small as 5 × 5 × 5 sites resulted only in a minor reduction of the energy transfer efficiency (typically by 5−10%).

4. Results and Discussion

4.1. Experimental Results. Determination of Photophysical Parameters. All parameters needed to calculate energy transfer rate constants between a DX pair at a given distance and angle using the Förster equation (eq 2) have been determined experimentally (Table 1) and will be used as input parameters

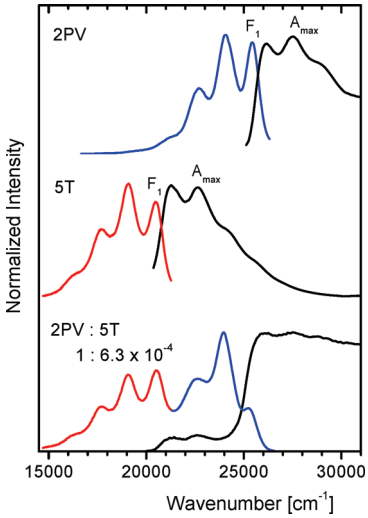

Figure 5. Normalized steady-state fluorescence emission (left) and excitation spectra (right) of different guests in PHTP. (Top) 2PV, center: 5T; (Bottom) 2PV:5T (1:6.3 × 10^{-4}).

for the simulations of energy transfer. Due to the light scattering nature and undefined thickness of the PHTP powder samples, it was not possible to obtain quantitative absorption spectra of the chromophores in PHTP. Instead, maximum extinction coefficients, ϵ_{max}, were determined in 1,4-dioxane. For the calculation of overlap integrals, J_{DX}, for 2PV-2PV and 2PV-5T (eq 3), absorption spectra were obtained from fluorescence excitation spectra, which were scaled by the ϵ_{max} given above. Similarly, fluorescence quantum yields were determined in cyclohexane solution. The treatment of the effect of the dielectric medium on the energy transfer process in a anisotropic medium is non-trivial.[38] We have chosen to use a typical value for the isotropic refractive index of a hydrocarbon ($n = 1.4$) and estimated that the error introduced on the overall energy transfer efficiency for rapid energy migration is likely to be small (see Section 4.2).

For the sake of comparison with previous data, the Förster radii for 2PV-2PV and 2PV-5T pairs have been calculated from the data in Table 1 using eq 6, inserting the isotropic value for fast rotational motion $\kappa^2_{DX} = 2/3$ and $n = 1.4$. Note that even though R_0 for homo-transfer is smaller than for hetero-transfer, it is still reasonably large compared to the typical interchromophore distances in the PHTP host structure. Thus, homo-transfer can be expected to play a significant role in the overall energy migration process.

Monitoring of Energy Transfer. 2PV/PHTP inclusion compounds doped with 5T exhibit efficient energy transfer from 2PV to 5T. Even at molar doping ratios below 10^{-3}, corresponding to an acceptor concentration of 5 × 10^{-4} M, experimental energy transfer efficiencies Φ_{ET} in excess of 0.6 are observed (see Figure 6). In the examined range of molar doping ratios, all donor decays from time-resolved experiments could be fitted by single-exponential functions. This is indicative of averaging the energy transfer rates through rapid diffusion of the excitation energy. Values of Φ_{ET} determined from steady-state experiments using eq 9 agree well with those obtained from time-resolved experiments on the same sample using eq 10. The time evolution of the fluorescence emission spectrum

(38) Knox, R. S.; van Amerongen, H. *J. Phys. Chem. B* **2002**, *106*, 5289.

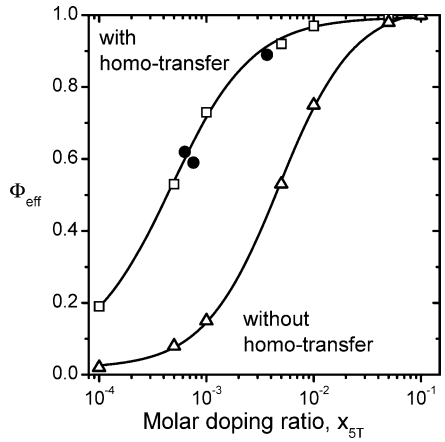

Figure 6. The energy transfer efficiency, Φ_{eff}, as a function of the molar doping ratio, x_{5T}. (●) Experimental data. MC simulation with random disorder and supramolecular correction for nearest neighbors without homo-transfer (△) and with homo-transfer (□). Solid lines are guides to the eye.

of typical sample upon excitation at 390 nm is shown in Figure 7. The characteristic rise and decay of the acceptor fluorescence is clearly recognizable. The meaning of the rise and the decay becomes evident only after examining the kinetics of the formation of the excited acceptor, $5T^*$. For single exponential donor decays, one finds:

$$[5T^*] = \left(\frac{\tau_{2PV/5T}}{\tau_{5T}} - 1\right)^{-1} \Phi_{ET}[2PV^*]_0(\exp(-\tau_{2PV/5T}) - \exp(-t/\tau_{5T})) \quad (13)$$

Thus, the decaying part of the trace corresponds to the acceptor decay only for $\tau_{2PV/5T} < \tau_{5T}$. It follows from eq 10 that, given $\tau_{5T} = 0.9$ ns and $\tau_{2PV} = 1.5$ ns (Table 1), this is the case for $\Phi_{ET} > 0.4$ (i.e., for all samples under investigation). At the same time, the rising part of the acceptor decay corresponds to the decay of the donor, which is clearly seen by comparing Figure 7a and b.

4.2. Simulation of Energy Transfer. Hopping Rate Constants. Rate constants for individual energy transfer steps between the molecules were calculated at the quantum-chemical level taking into account the full electronic structure of the chromophores for a series of distances and compared to the results of the Förster PDA model (Figure 4). As reported in other works,[3,40] it is found that the rate constants for energy transfer to nearest neighbors are not well accounted for by PDA, owing to the small intermolecular separations in comparison to the molecular sizes. For *intra*channel transfer, the PDA *under*-estimates the rate constant by a factor of more than two at a center-to-center distance of 2 nm. For *inter*channel transfer (between neighboring channels), however, the rate constants are *over*estimated at center-to-center distances below 1.7 nm. Thus, depending on the population of the neighboring channels, the PDA may under- or overestimate the overall transfer rates and, certainly, give an incorrect picture of the relative roles of *intra*- and *inter*channel transfer processes (though cancellation of errors might accidentally lead to, e.g., reasonable diffusion lengths).

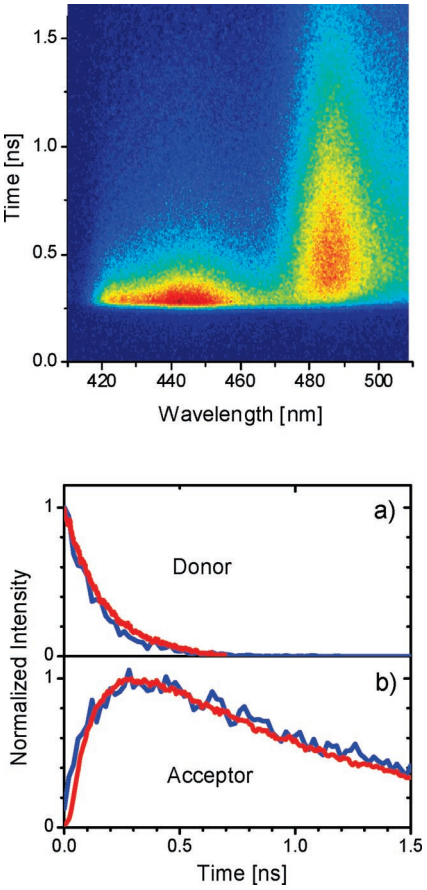

Figure 7. (Top) Experimental, spectral and time-resolved 2D plot of the donor fluorescence decay and the acceptor rise and decay upon excitation at 390 nm ($x_{5T} = 3.7 \times 10^{-3}$). (Bottom) (a) Comparison between the simulated donor decay (blue) and the experimental donor fluorescence decay at 440 nm (red) and (b) between the simulated acceptor time trace (blue) and the experimental acceptor fluorescence rise and decay at 550 nm (red).

The Energy Diffusion Process. In this section, we use the different models introduced in Section 2 for simulating the ET efficiencies, as well as the donor and acceptor decays. We start with the analytical expressions eqs 7 and 8, which describe point dipoles in an isotropic system, without and with energy migration among donors, respectively. By applying the MC approach described in Section 3.2, we are able to impose the static hexagonal order of the PHTP systems. In a further step, we introduce positional disorder with respect to neighboring channels. On the other hand, energetic disorder, which plays an important role in polymeric samples,[3] was not considered in the calculations. This is justified by the use of oligomers and their confinement in the channels which imposes a narrow distribution of energetic sites. This is confirmed by the small bandwidth of the optical spectra compared to the one in solution, see Figure 5.[36] Finally, we compare the results of MC simulations using the PDA (eq 2) and the distributed monopole approach (eq 5) for the calculation of the rate constants k_{DX}. All calculations are performed for a molar doping ratio of $x_{5T} = 10^{-3}$. The results are summarized in Table 2.

4.2.1. Isotropic Models. All parameters needed to calculate energy transfer rate constants between a DX pair at a given distance and angle using the Förster equation (eq 2) have been determined experimentally (Table 1) and are used as input parameters for the following analytical calculations of energy transfer.

(39) Oelkrug, D.; Egelhaaf, H.-J.; Gierschner, J.; Tompert, A. *Synth. Met.* **1996**, *76*, 249.
(40) (a) Wong, K. F.; Bagchi, B.; Rossky, P. J. *J. Phys. Chem. A* **2004**, *108*, 5752. (b) Grage, M. M.-L.; Zaushitsyn, Y.; Yartsev, A.; Chachisvilis, M.; Sundström, V.; Pulleritis, T. *Phys. Rev. B.* **2003**, *67*, 205207.

Table 2. Comparison between Overall Energy Transfer Efficiencies, Φ_{ET}, as Calculated With and Without Donor−Donor (DD) Transfer Using the Static and Rapid Diffusion Limits, Respectively, of Standard Isotropic Models and Using Monte Carlo Simulations with a Perfect Hexagonal Lattice (MC PDA), Disorder along the Channel Axis (MC PDA and Disorder), and Supramolecular Treatment (MC DMA and Disorder)[a]

	Φ_{ET} without DD	Φ_{ET} with DD	predicted fraction of *intra*channel transfer steps
1a. Isotropic ($\kappa^2 = 2/3$)	0.21 (static)	0.84 (rapid)	–
1b. Isotropic ($\kappa^2 = 0.476$)	0.18 (static)	0.79 (rapid)	–
2. MC PDA	0.14	0.81	20%
3. MC PDA and disorder	0.15	0.68	40%
4. MC DMA and disorder	0.15	0.73	70%

[a] Molar doping ratio was $x_{5T} = 1 \times 10^{-3}$. For comparison, the interpolated experimental value as taken from Figure 6 of Φ_{ET} is ~0.7. The fraction of the homo-transfer steps predicted to be *intra*channel is also shown.

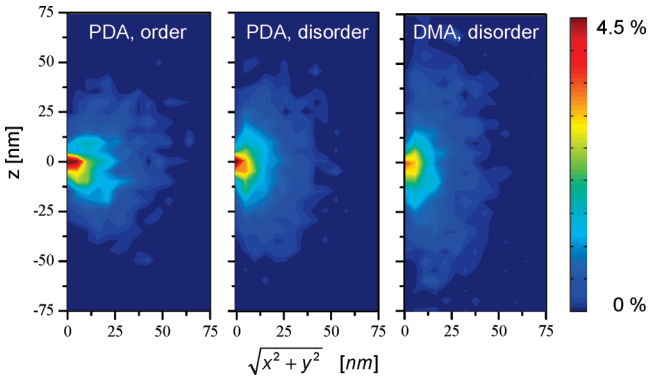

Figure 8. Probability $4\pi r^2 \rho$ of decay as a function of the distance, parallel and perpendicular to the channel axis, to the site of initial excitation, as obtained from 2500 individual trajectories of the MC calculations for $x_{5T} = 10^{-3}$ for different models. (Left) point-dipole approximation (PDA), hexagonal symmetry. (Center) PDA, positional disorder along *z*. (Right) positional disorder, including quantum-chemical correction (DMA).

Förster's isotropic model in the *static limit* (eq 7) leads to very small energy transfer efficiencies ($\Phi_{ET} \approx 0.2$) far below the experimental values. On the other hand, the isotropic models for both frozen and rapidly rotating dipole moments in the *rapid-diffusion limit* (eq 8), assuming a smallest encounter distance of $r_c = 1.5$ nm, yield Φ_{ET} values close to, but systematically higher than the experimental values. We will return to the significance of this in the discussion of excitation diffusion.

4.2.2. Perfect Hexagonal Lattice, Point-Dipole Approximation. The MC simulations, similar to the analytical isotropic model, yield very small Φ_{ET} values when homo-transfer is neglected. In contrast, values of Φ_{ET} closer to the experimental ones are obtained when allowing for jumps between donors. An excitation was found to undergo an average of 300 homo-transfer steps before decaying. 98% of homo-transfer steps were to the first shell of molecules surrounding the excitation and 80% to a molecule in a neighboring channel (*inter*channel transfer). In the perfect hexagonal lattice, this corresponds to *quasi*-2D diffusion of the excitation in the xy-plane. The directionality of energy migration is visualized in Figure 8, showing the distance covered by the excitations from the site of initial excitation to the site of decay, averaged over a few thousand individual MC trajectories.

4.2.3. Positional Disorder Along the *z*-Axis. X-ray diffraction data of PHTP inclusion compounds suggest that the guest molecules are not perfectly ordered between neighboring channels, but rather displaced relative to each other,[15] because no correlation is expected between guest molecules in different channels, see Figure 1. This disorder can be represented by randomly displacing the guest molecules in the neighbor channels by up to half a molecule length in the channel direction. Because the rate constant for *inter*channel energy transfer has a maximum at an angle of $\theta = 0°$, corresponding to the side-by-side position, but vanishes at around $\theta = 55°$ in the PDA approach (eq 4 and Figure 4), this type of *inter*channel disorder results in a reduction of the average rate constant for *inter*-channel energy transfer. The result is evident as a slight decrease of the overall efficiency and leads to a significant increase in the proportion of *intra*channel homo-transfer steps from 20% to 40%.

4.2.4. Quantum-Chemical Correction for Closest Neighbors (Distributed Monopole Approach, DMA). Surprisingly, overall transfer efficiencies calculated using the supramolecular approach do not differ appreciably from those calculated using the PDA. In other words, the failure of the PDA at small distances (Section 4.2.1) does not lead to false predictions of the overall transfer efficiency. This is mainly due to the specific geometry of the hexagonal lattice, where the *average intra*-channel rate constant is underestimated by approximately the same amount as the *average inter*channel rate constant is overestimated (i.e., there are only two *intra*channel neighbors compared to six *inter*channel neighbors). Despite the apparent good performance of the PDA, it is important to note that, as a consequence of its limitations described above, the PDA yields an incorrect picture of the mechanism of excitation diffusion by overestimating the role of *inter*channel transfer. Indeed it is found that more than 70% of all homo-transfer steps are *intra*channel (as opposed to 40% for PDA), so that excitation diffusion occurs preferentially along the channel axis, though not fully in one dimension, see Figure 8.

Using only experimental input parameters for the simulations, excellent agreement between the simulated donor and acceptor decays and the experimental data was found (Figure 7b). The simulations reproduce the rise and decay characteristics of acceptor fluorescence as well as the expected correspondence between the acceptor rise time and the donor decay time.

Let us now examine the excitation migration process further. Excitation diffusion coefficients were quantified through their simulated mean square displacements.[41]

$$6Dt = \langle |r_i(t) - r_i(0)|^2 \rangle \qquad (14)$$

The radial diffusion coefficient was estimated to be $D_{DD} = 3 \times 10^2$ nm^2 ns^{-1} (for comparison, this is 2 orders of magnitude faster than typical gas diffusion in a liquid at room temperature). Thus, within the lifetime of the excitation in the absence of traps, the mean radial diffusion length of the excitation, $d_{dif} = (6D\tau_{2PV})^{1/2}$ is 50 nm. This is comparable to the typical values reported for thin films of organic molecules;[42] for instance, a diffusion length of ~65 nm has been measured in polycrystalline

(41) Allen, M. P.; Tildesley, D. J. *Computer Simulations of Liquids*; Oxford University Press: New York, 1987.
(42) Peumans, P.; Yakimov, A.; Forrest, S. R. *J. Appl. Phys.* **2003**, *93*, 3693.

pentacene used as donor in C_{60}-based photovoltaic junctions.[43] Much smaller values (on the order of 10 nm) are usually achieved in conjugated polymers mostly as a result of their much broader energetic distributions, hence low-energy sites act as traps for excitation diffusion.[44] For comparison, the mean distance between two acceptor molecules, d_{AA}, is 20 nm at $x_{5T} = 1 \times 10^{-3}$. The distribution of distances between the initial excitation and the site of decay at this molar doping ratio is shown in Figure 8. Under these conditions, the mean radial diffusion length of the excitation, $d_{dif} = (6D\tau_{2PV/5T})^{1/2}$, reduces to 25 nm. Keeping in mind that $d_{dif} \gg d_{AA}$ defines the rapid-diffusion limit, we investigated the effect of excitation diffusion on Φ_{ET} by systematically varying the donor−donor spectral overlaps, J_{DD}, in the simulation. With increasing J_{DD}, Φ_{ET} reaches a plateau and above $J_{DD} = 5 \times 10^{31}$ nm^6 mol^{-1}, corresponding to $D_{DD} = 3 \times 10^4$ nm^2 ns^{-1}, Φ_{ET} no longer depends on J_{DD}. In this limit, corresponding to the rapid-diffusion limit, Φ_{ET} is 10% larger than at the experimental conditions ($J_{DD} = 1 \times 10^{31}$ nm^6 mol^{-1}). The weak dependence of Φ_{ET} on J_{DD}, and ultimately on k_{DD}, near the rapid-diffusion limit is also the reason for the observed successful prediction of Φ_{ET} by the simple isotropic models. From the evaluation of the simulated donor-decay curves, it is found that in the proximity of the rapid-diffusion limit, donor decays can be represented by a single-exponential function. In fact, strongly non-exponential decays of the donor fluorescence first became evident at J_{DD} values which are 50% smaller than the experimental J_{DD}. Therefore, the experimentally observed single exponential donor decays are in full agreement with excitation diffusion close to the rapid-diffusion limit. It is interesting to note that this differs significantly from the situation in end-capped conjugated polymers where excitation decay is non-exponential and the energy transfer to the acceptor end-groups is diffusion limited.[45]

In summary, the mechanism of energy transfer in the PHTP nanochannel compound consists of (i) rapid diffusion of the excitation energy to a site neighboring an acceptor site followed by (ii) energy transfer to the acceptor site. Taking into account the features of the real system (i.e., disorder along the channel axis as well as the short interchromophore distances), the simulations show that the diffusion process occurs preferentially along the channel axis. The mechanism is supported by the excellent agreement between the energy transfer efficiencies Φ_{ET} obtained by experiment and those predicted from Monte Carlo simulations in the examined range of molar doping ratios (Figure 6). Furthermore, without the use of any fitting parameters, both the experimental donor decay and the acceptor rise and decay kinetics are accurately reproduced by the simulations (Figure 7). It is important to note that the preferential intra-channel ET mechanism observed in both the present PHTP host−guest compound and in zeolite L (see ref 10) differs significantly from polymer samples, where the energy is transferred preferentially between the chains.[45] The reason for this difference is found in the much smaller interchain separation in the polymer (0.4 nm) compared to the inter-channel separation in PHTP (1.5 nm) or zeolite L (1.8 nm).

5. Conclusions

A Monte Carlo method for simulating three-dimensional energy migration in a large, periodic lattice with multiple energy accepting sites was developed. Using this method, a full simulation of a highly dense three-dimensional multiple acceptor energy transfer system using rate constants calculated at the quantum-chemical level for interactions at short interchromophore distances was achieved yielding information about the directionality of the energy migration.

The method was applied to a system of highly luminescent chromophores included in the channels of a well-ordered, self-assembled, nanostructured host−guest system. The organic host structure, PHTP, forms nanochannels around the chromophores, in this case an oligo-phenylene vinylene, 2PV, allowing for very high chromophore concentrations while still maintaining the solution-like optical properties, namely their high luminescence. The PHTP/2PV structure was doped with small amounts of an oligothiophene, 5T, acting as the energy accepting chromophores. The well-defined geometry of the PHTP nanochannels allowed for a full comparison between simulated and experimental data.

With only experimental input data and no fitting parameters, the simulations reproduce both the experimental donor and acceptor decays. Excellent agreement with the overall transfer efficiencies is also found. The simulations show that in the 2PV/PHTP system the energy transfer efficiency from donor species to acceptor species is significantly enhanced by diffusion of the excitation energy through a series of donor to donor homotransfer steps. As a result, even at low acceptor concentrations (5×10^{-4} M), energy transfer efficiencies in excess of 60% and exciton diffusion lengths of $d \approx 25$ nm are achieved. The rapid diffusion of the excitation energy leads to averaging of the effective donor−acceptor energy transfer rate constants and, therefore, single-exponential decays of the donor fluorescence. The true directionality along the channel axis is revealed only by an atomistic description of the interactions between neighboring chromophores using the distributed monopole approach. The developed method can be readily applied to any ordered system and may yield valuable insight into the dynamics of excitation diffusion in condensed systems provided they fall into the weak coupling regime.

Acknowledgment. This work was supported by the European Commission (EC) through the Human Potential Program (Marie-Curie Research Training Networks NANOCHANNEL Contract No. HPRN-CT-2002-00323, and NANOMATCH, MRTN-CT-2006-035884) and by the EC STREP project MODECOM (NMP−CT-2006-016434). The work in Cagliari has been partially funded through FIRB projects (Synergy-FIRB-RBNE03S7XZ and FIRB-RBAU01N449). D.B. and J.C. are Research Associates of the FNRS. We thank Gregory Scholes, Toronto, Canada, and Dmitry Khoptyar, Tübingen, Germany, for useful discussions.

JA0714437

(43) Yoo, S.; Domercq, B.; Kippelen, B. *Appl. Phys. Lett.* **2004**, *85*, 5428.
(44) See e.g. Markov, D. E.; Tanase, C.; Blom, P. W. M.; Wildeman, J. *Phys. Rev. B* **2005**, *72*, 045217.
(45) Hennebicq, E.; Pourtois, G.; Scholes, G. D.; Herz, L.M.; Russel, D. M.; Silva, C.; Setayesh, S.; Grimsdale, A. C.; Müllen, K.; Brédas, J. L.; Beljonne, D. *J. Am. Chem. Soc.* **2005**, *127*, 4744.